Hindawi
Advances in Civil Engineering
Volume 2018, Article ID 5350315, 14 pages
https://doi.org/10.1155/2018/5350315

Research Article

Bending Resistance of Composite Sections with Nonductile Shear Connectors and Partial Shear Connection

Svetlana M. Kostic and Biljana Deretic-Stojanovic

Faculty of Civil Engineering, University of Belgrade, Belgrade 11000, Serbia

Correspondence should be addressed to Svetlana M. Kostic; svetlana@grf.bg.ac.rs

Received 12 April 2018; Revised 3 July 2018; Accepted 27 August 2018; Published 24 September 2018

Academic Editor: Pier Paolo Rossi

The paper presents the nonlinear section analysis for composite steel-concrete beams with different degrees of shear connection. The analysis is fiber based, i.e., integration over the cross section is performed numerically, and any uniaxial nonlinear material model can be assigned to the steel and concrete parts of the cross section or to the reinforcement bars. The analysis assumed full interaction between steel and concrete and therefore, is suitable for analysis of composite steel-concrete beam cross sections with nonductile shear connectors. Its accuracy is verified on few experimental results. The presented section analysis is used in the parameter study in order to evaluate different methods proposed by design codes for determining the bending moment resistance of composite cross sections with nonductile shear connectors and different degrees of shear connection. The following effects are considered: variation of concrete and steel material models, presence of slab reinforcement, and creep of concrete. Special attention is paid on two different constructional methods: propped and unpropped. The weaknesses of the simplified design method in determining bending moment resistance are identified and recommendations for practical design analysis are formulated.

1. Introduction

Composite steel-concrete structures are in increasing use over the last several decades [1–3]. In composite beams, with typical cross sections as shown in Figure 1, composite action between the concrete slab and steel section is achieved through the shear connectors placed at the steel-concrete interface. Behaviour of these beams is governed by the nonlinear behaviour of each constituent part: steel section, concrete slab, and shear connectors [4].

Considering shear connectors, the bending resistance of a composite section depends on the type of the used shear connectors, their characteristics, and the design of the shear connection. Depending on the strength of the shear connection, shear connections are classified as full and partial. The use of partial shear connection is common in cases when ultimate strength of the composite section does not govern the design. For example, when stiffness of the composite beam is determined from the deflection criteria or, in unpropped construction, when dimensions of the steel beam are determined from a critical stage during construction.

According to the shear connectors' ductility, connectors are classified as ductile and nonductile [1]. This classification is based on the load-slip characteristics of shear connectors. Behaviour of beams with ductile and nonductile shear connectors differs significantly and, for this reason, in design codes, different types of analysis are proposed. Bending resistance of the composite section with ductile connectors, that also satisfy additional requirements about connector dimensions and distribution in the shear connection, is determined using the simple equilibrium method and the rigid plastic analysis [5, 6]. On the other side, when shear connectors do not satisfy the prescribed ductility requirements either because of their type or because of the design of the shear connection, bending resistance cannot be determined in accordance with the rigid plastic analysis. In these cases, the elastic analysis or the nonlinear analysis needs to be used [6].

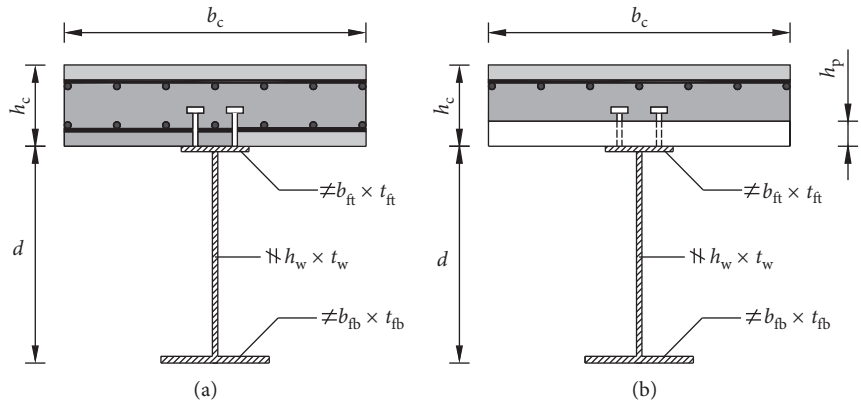

Figure 1: Typical cross sections of composite beam with (a) full concrete slab and (b) composite slab (on profiled steel sheeting).

To date, there are several experimental and numerical studies that address the analysis of composite beams with partial shear connection and ductile shear connectors [4, 7–13]. Most of the numerical models are either 3D models that use solid finite elements or 1D finite element models. The 3D numerical models [14] are very powerful and accurate in predicting both global behaviour of composite beams and local behaviour such as stress concentrations near shear connectors and local bucking. However, these models are computationally very expensive and not suitable for ordinary engineering practice. Among 1D finite elements, the most common approach is the fiber-based element that uses different nonlinear uniaxial constitutive relations for steel, concrete, and shear connectors [4, 7, 10, 12]. Although these elements find a balance between computational efficiency and accuracy, still, their use in practice is very limited. This mostly comes from the fact that these models are not easily available and, in order to be correctly used, the advanced knowledge of nonlinear structural analysis is required. From these reasons, the study presented in this paper explains the simple nonlinear model for calculation of bending resistance of beams with nonductile shear connectors and partial shear connectors that is suitable for use in practice. The motivation for the study also comes from the fact that nonductile shear connectors find their use in both bridges and buildings. Aside, the general trend of the use of filigree constructional elements in civil engineering structures initiates development of new types of shear connectors that do not satisfy the ductility requirements prescribed by design codes [15] and cannot be analysed as ductile shear connectors. However, there are only few experimental and numerical studies that address this problem [16].

The nonlinear analysis method presented in this paper can be used for determining the bending resistance of a composite section with nonductile shear connectors and different degrees of shear connection. The method is simple and suitable for use in engineering practice. It is based on the fiber-section analysis [17] and can be used in conjunction with any uniaxial material constitutive relations for constructional steel, concrete, and reinforcement. The method takes into account the construction method: propped and unpropped. The proposed numerical model is validated against the available experimental investigations and more complex numerical models by other authors. This model is then used to carry out a series of parametric analyses on a range of steel-concrete beam composite sections. The results are also compared with the simplified method prescribed by most design codes and limitations of the simplified method are identified.

2. Overview of the Design Code Analysis Methods for Nonductile Connectors

The shear connectors are classified as ductile and nonductile according to their load-slip curves (Figure 2).

Referring to the shear connection, the terms full and partial shear connection are used depending on the strength of the shear connection. The full shear connection implies that the strength of the shear connection is high enough and the maximum moment of resistance governs the ultimate load. Therefore, use of more shear connectors will not increase the value of the ultimate load. When less shear connectors are used, the maximal moment of resistance cannot develop, and the shear connection is denoted as partial [2, 16]. Finally, when there are no shear connectors, the steel beam alone determines the ultimate loads. Therefore, beams with partial shear connection fails because of the failure of the shear connectors.

In order to calculate the ultimate load of the beam, the bending resistance of the composite steel-concrete cross section needs to be determined for the critical beam cross sections. Behaviour of beams with partial shear connection differs significantly depending on the used number of shear connectors and their deformation characteristic. When ductile shear connectors are used, as soon as the ultimate load of the shear connector is reached, connectors further deform and slip may occur at the steel/concrete interface. Consequently, neutral axes in the steel beam and concrete slab differ [16]. In these cases, according to design codes, bending resistance of composite section with ductile connectors can be determined using the simple equilibrium method and the rigid plastic analysis [5, 6, 16]. The connectors also need to satisfy additional requirements about connector dimensions and position in the shear connection. The longitudinal shear force at the failure is equal to the sum of the resistances of the shear connectors. Several experimental and numerical studies confirmed this approach [11, 18–20].

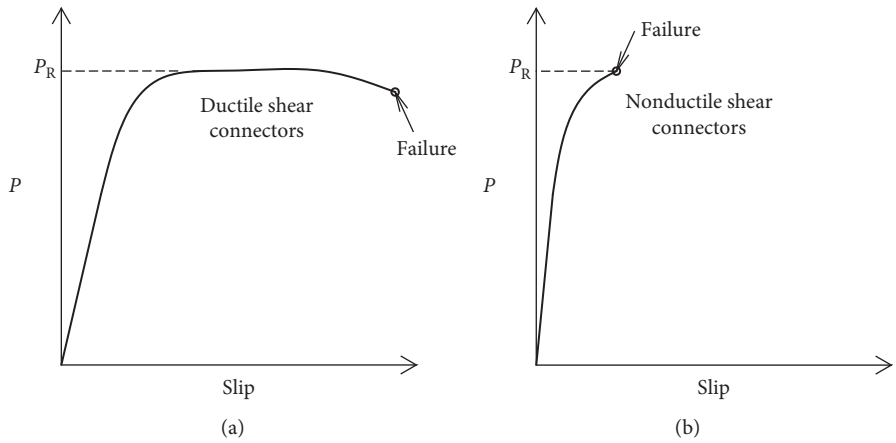

Figure 2: Typical load-slip relations for (a) ductile and (b) nonductile shear connectors.

When nonductile rigid shear connectors are used, once the ultimate load of the shear connectors is reached, the ultimate load of the beam is attained since the connectors do not have any deformation capacity. At failure, the neutral axes of the steel beam and the concrete slab coincide. The longitudinal shear force at the failure is equal or smaller to the sum of the resistances of the shear connectors depending on their distribution along the shear span. In reality, nonductile shear connectors are not absolutely rigid, and some slip does occur at the steel-concrete interface, especially for lower degrees of the shear connection [16]. However, this slip is very small and, for being on the safe side, design codes suggest to ignore it. This is also confirmed by experimental investigations [16]. Therefore, bending resistance of composite section with nonductile connectors cannot be determined in accordance with the rigid plastic analysis [21]. Design codes allow either overconservative elastic analysis or nonlinear analysis to be used [6]. In addition, it should be noted that there are some cases when bending resistance of beams with ductile shear connectors cannot be obtained according to the rigid plastic analysis: for example, when shear connectors do not satisfy the prescribed ductility requirements either because of their type, ductility, or the design (distribution and position in the shear connection).

In nonlinear analysis, the nonlinear constitutive relations for constructional steel, concrete, and reinforcement need to be taken into account. In addition, the analysis can take into account the real load-slip behaviour of connectors. Since this relation is not always available and since the calculation of slip at the steel-concrete interface involves use of advanced numerical models, the design codes (Eurocode 4 [22], for example) suggest to completely ignore slip at the interface when nonductile shear connectors are used. Also, the preloading of the steel beam and the effects due to creep and shrinkage should be taken into account.

The above-described nonlinear analysis is not suitable for practical applications. Therefore, design codes suggest the simple procedure, as shown in Figure 3.

This method assumes that relation between the bending moment resistance and the degree of shear connection η is linear for η greater than the degree of shear connection that corresponds to the elastic moment resistance $M_{el,Rd}$. The degree of shear connection η is defined as the ratio between the design value of the compressive force in the concrete slab (N_c) and the design value of the compressive force in the concrete slab with full shear connection (N_{cf}). The full shear connection ($\eta = 1$) is defined as connection with number of shear connectors sufficient to achieve the full-plastic bending resistance of composite section, $M_{pl,Rd}$. On the other side, in the partial shear connection, the number of shear connectors is lower than that required for the full plastic resistance $M_{pl,Rd}$ to be achieved, and the bending resistance reduces to M_{Rd} which is smaller than $M_{pl,Rd}$. As Figure 3 shows, different curves correspond to the propped and unpropped construction method. The elastic moment resistance and the force in the concrete slab that correspond to $M_{el,Rd}$ are denoted with $M_{el,Rd,p}$, $M_{el,Rd,u}$, $N_{c,el,p}$, and $N_{c,el,u}$, respectively, for propped and unpropped structures. For unpropped structures, $M_{a,Ed}$ is the design bending moment acting on the steel section alone.

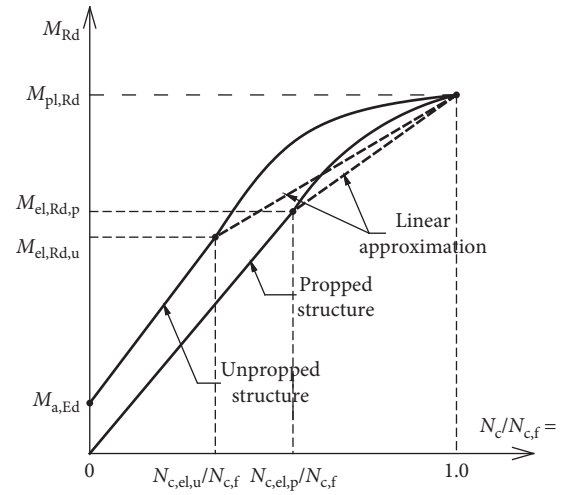

Figure 3: Bending resistance vs. degree of shear connection for propped and unpropped structures: nonlinear relation and approximate bilinear relation.

3. Section Fiber Analysis

In order to evaluate the analysis methods described in the previous section, the following numerical model for nonlinear section analysis is defined. The analysis is based on the fiber section model and adopts the assumption of the linear strain distribution over the composite section height (no slip between the steel section and concrete slab). The considered cross section from Figure 1(a) consists of concrete slab and steel section. The section is divided into a number of layers since the performed analysis considers only bending about strong axis. For the biaxial bending cases, the discretization into fibers would be required. It should be noted that different sections, for example, sections with composite slab on profiled steel sheeting or with different steel sections, could also be analysed in the same manner. Since the use of nonductile shear connectors is commonly related to sections with full concrete slab and I steel section, the presented study is focused on the cross section from Figure 1(a).

The ductile shear connectors can be uniformly spaced along the critical length since enable redistribution of longitudinal shear force over the length. On the contrary, optimal design with the nonductile connectors adopts the distribution of the shear connectors that is based on the distribution of the longitudinal shear force [16]. This way, the longitudinal shear force at failure becomes equal to the sum of the resistances of the shear connectors. In practice, this distribution is usually determined from elastic analysis. For other distributions of shear connectors, the ultimate load is reached as soon as the longitudinal shear force on the heaviest loaded connector equals its resistance. In the presented study, it is assumed that shear connectors are optimally distributed. The same section bending resistance curve, with correctly calculated longitudinal shear force at failure, can be used for other distributions of shear connectors as well.

The nonlinear uniaxial constitutive stress-strain models are assigned to each layer. In the validation study, the nonlinear concrete material model prescribed by Eurocode 2 is assigned to concrete layers (Figure 4(a)).

The relation between the concrete stress σ_c and strain ε_c in compression is defined by positive values in compression

$$\frac{\sigma_c}{f_c} = \frac{k\left(\varepsilon_c/\varepsilon_{c1}\right) - \left(\varepsilon_c/\varepsilon_{c1}\right)^2}{1 - (k-2)\left(\varepsilon_c/\varepsilon_{c1}\right)}, \tag{1}$$

where ε_{c1} is the strain peak stress,

$$\varepsilon_{c1}\,(‰) = \min\begin{cases} 2.8, \\ 0.7\left[f_c\right]^{0.31}, \end{cases} \tag{2}$$

f_c is the peak concrete stress, and

$$k = \frac{1.05E_c\left|\varepsilon_{c1}\right|}{f_c}. \tag{3}$$

The concrete modulus E_c in GPa is found as (f_c is in MPa)

$$E_c = 22\left[\frac{f_c}{10}\right]^{0.3}, \tag{4}$$

and the concrete ultimate strain ε_{cu1} is

$$\varepsilon_{cu1}\,(‰) = \min\begin{cases} 3.5, \\ 2.8 + 27\left[\dfrac{98 - f_c}{100}\right]^4. \end{cases} \tag{5}$$

Concrete strength in tension is neglected.

The simple elastic and perfectly plastic relation for reinforcement is adopted (Figure 4(b)) with reinforcement yield strength denoted as f_{yr}. Hardening was not included because there were no available data about it in the studied examples.

The simple three-linear constitutive relation with strain hardening is adopted for constructional steel (Figure 4(c)). In this figure, E_s denotes Young's modulus of steel, f_y is the yield strength, f_u is the ultimate strength, and ε_y is the yield strain. The onset of hardening is defined through the coefficient μ_1 as $\mu_1\varepsilon_y$, and similarly, the ultimate strain is defined through coefficient μ_2 as $\mu_2\varepsilon_y$. The hardening modulus is E_{sh}. The same relations in tension and in compression are assumed.

In addition, it is assumed that local instability effects such as buckling of the steel section are prevented. The proposed analysis considers both construction methods, propped and unpropped. Creep effects are taken into account through the modular ratio n in calculation of the elastic moment resistance $M_{el,Rd}$, and this effect is discussed latter in the parameter analysis. Shrinkage effects are neglected.

In the first analysis step, depending on the construction method, initialization of stresses (and strains) is done. For propped construction, stresses in all layers are initialized to zero. For the unpropped construction method, stresses corresponding to the moment M_a acting on the steel beam alone are assigned to the steel section layers, while stresses in other layers are assigned to zero. In the second step, the linear strain distribution over the height of the composite cross section is assumed. The corresponding section deformation vector for 2D analysis is denoted with **e**:

$$e = \begin{bmatrix} \varepsilon_a \\ \kappa \end{bmatrix}, \tag{6}$$

where ε_a is the strain at the origin of the reference axis and κ is the curvature (Figure 5).

In order to calculate the section bending resistance curve for all degrees of the shear connection (i.e., for η between 0 and 1), the strains at the top of the concrete, ε_{ct} (Figure 5) need to change between 0 and the ultimate value, ε_{cu1}. Therefore, the algorithm consists of two phases, one is incrementation of the strains at the top of the concrete slab, ε_{ct}, and the other are iterations. During iterations, for the constant strain at the top of the concrete, strain at the bottom of the steel flange, ε_{sb}, is changed until the equilibrium equation for the axial force is satisfied:

$$N - N(e) = 0. \tag{7}$$

In Equation (7), N is the given axial force which is equal to 0 for the considered pure bending problem; $N(e)$ is the

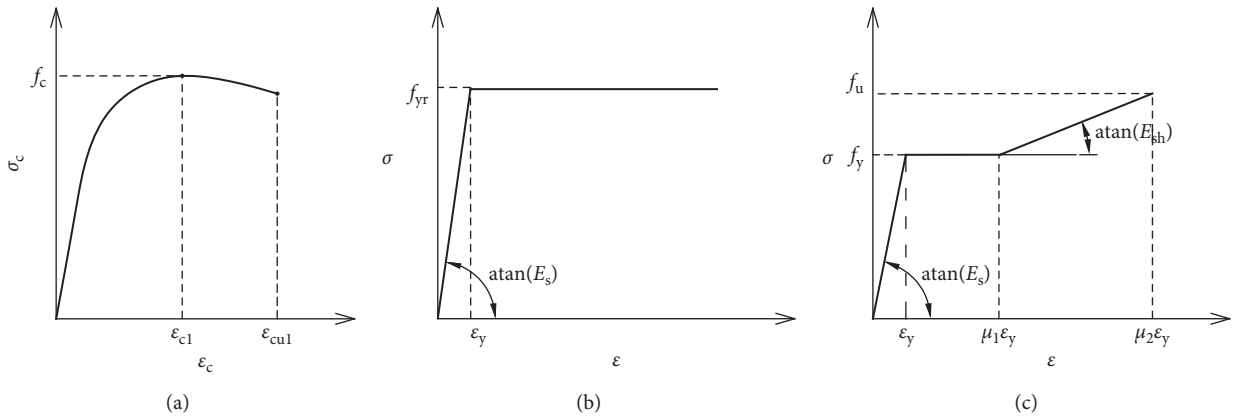

Figure 4: Constitutive relations for (a) concrete, (b) reinforcement, and (c) steel.

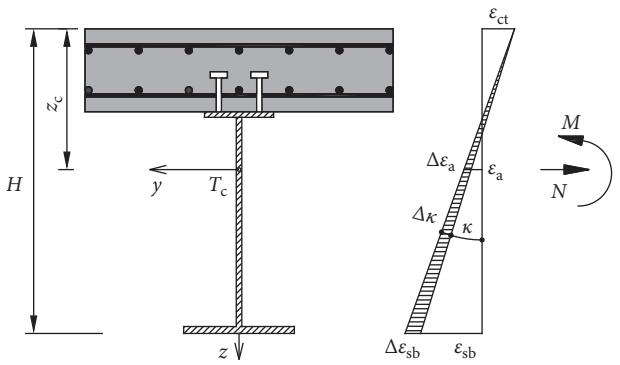

Figure 5: Strain distribution and its correction during iterations.

axial force that corresponds to the assumed section strains, e. The force $N(e)$ together with the bending moment $M(e)$ is determined for each section deformation vector e (i.e., for each strain distribution) by integration (i.e., summation) over the cross section:

$$N = \sum_{i=1}^{N_{\text{layer}}} (\sigma_i + \sigma_{0i}) A_i,$$
$$M = \sum_{i=1}^{N_{\text{layer}}} (\sigma_i + \sigma_{0i}) z_i A_i, \tag{8}$$

where σ_i are stresses at midpoints of all layers determined from known constitutive relations and the considered strain distribution. The total number of layers is N_{layer} and σ_{0i}, z_i, and A_i are, respectively, initial stress, z coordinate, and area of layer i. In the next step, checking of whether the equilibrium Equation (7) is satisfied (up to a tolerance) is done. If this condition is satisfied, the resulting force in the concrete slab N_c is calculated through integration (i.e., summation) over the concrete slab layers only. Finally, the corresponding degree of shear connection η is determined by dividing this value with N_{cf}.

At the start of the analysis, $\varepsilon_{ct} = 0$ is assumed. During the incrementation phase, with an increment in concrete strains $\Delta\varepsilon_{ct}$, the increment in strain at the bottom of the steel flange, $\Delta\varepsilon_{sb}$, is determined as follows:

$$\Delta\varepsilon_{sb} = \left[\frac{\partial N}{\partial \varepsilon_a}\frac{z_c}{H} - \frac{\partial N}{\partial \kappa}\frac{1}{H}\right]^{-1} \cdot \left(N - N(e) - \left(\frac{\partial N}{\partial \varepsilon_a}\left(1 - \frac{z_c}{H}\right) + \frac{\partial N}{\partial \kappa}\frac{1}{H}\right)\Delta\varepsilon_{ct}\right), \tag{9}$$

$$\varepsilon_{sb,new} = \varepsilon_{sb} + \Delta\varepsilon_{sb}, \tag{10}$$

where partial derivatives $\partial N/\partial\varepsilon_a$ and $\partial N/\partial\kappa$ are elements of the first row of the section tangent stiffness matrix, H denotes the total height of the composite section, and T_c is the origin of the reference axis with its z_c position from the top of the concrete slab. For the considered problem, since there is no axial force, the origin of the coordinate system can be placed anywhere in the plane of the cross section. One interesting choice is at the top of the concrete slab since, in this case, ε_a becomes ε_{ct}, and variation of strain at the bottom of the steel section produces only changes in the curvature. However, the solution given here is shown for other positions of the origin of the reference axis.

If the equilibrium Equation (7) with $N(e_{new})$ is not satisfied up to a tolerance, iterations start and strain at the bottom of the steel section, ε_{sb}, changes, while the strain ε_{ct} keeps unchanged. During these iterations, increment in the strain $\Delta\varepsilon_{sb}$ is calculated as follows:

$$\Delta\varepsilon_{sb} = \left[\frac{\partial N}{\partial \varepsilon_a}\frac{z_c}{H} - \frac{\partial N}{\partial \kappa}\frac{1}{H}\right]^{-1} (N - N(e_{new})). \tag{11}$$

Expressions from Equations (9) and (11) come from expansion of Equation (7) into a Taylor series and after its linearization. The process converges fast. For example, for the axial force tolerance of 10^{-12}, the solution is obtained after 3 to 4 iterations.

Once a convergence is achieved, after incrementation of the strain ε_{ct}, the state determination process repeats starting with the ε_{sb} strain from the last converged state. The flowchart of the procedure is shown in Figure 6.

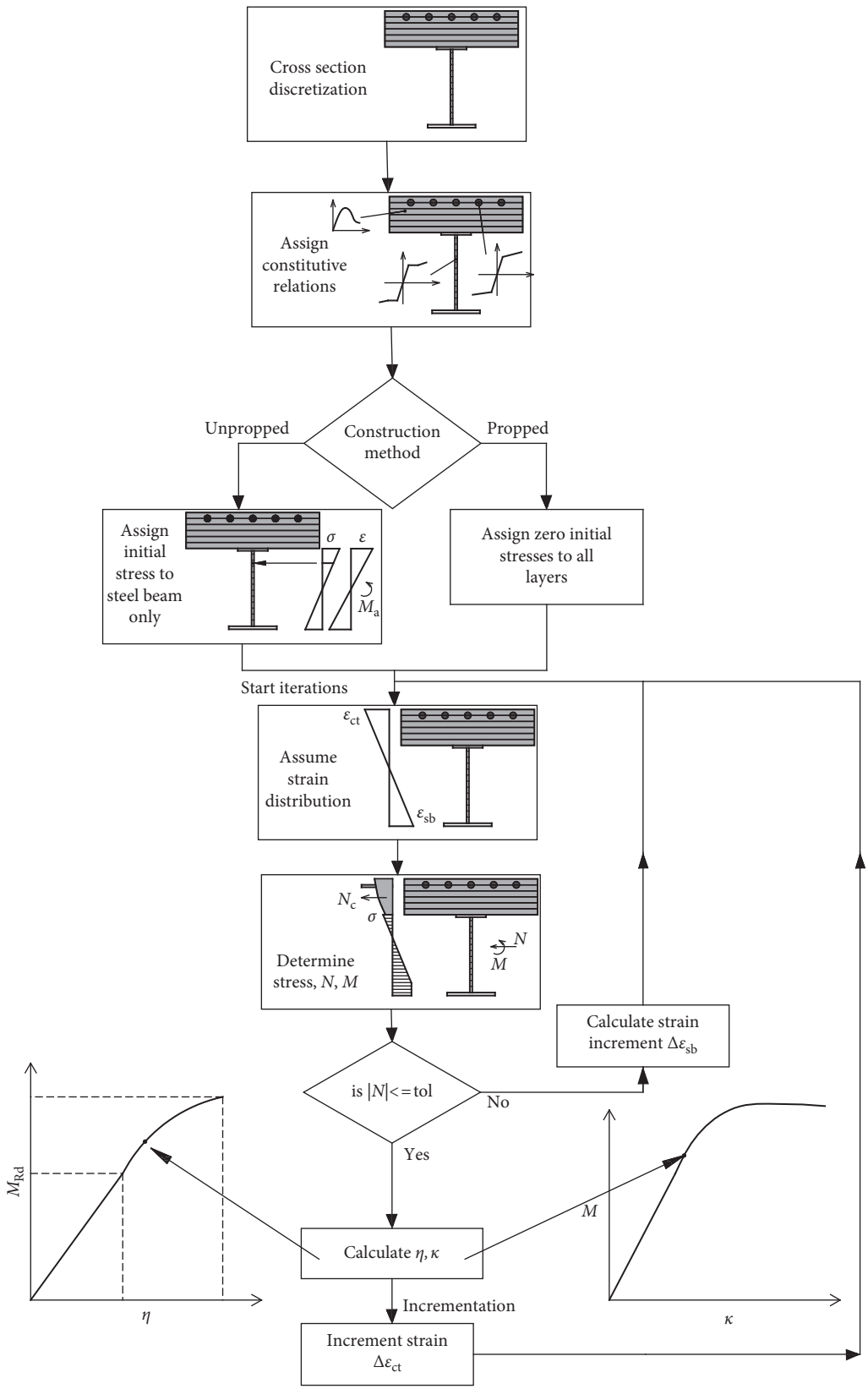

Figure 6: Algorithm of the nonlinear section analysis.

4. Verification of the Proposed Method for Section Analysis

In order to verify the section analysis method proposed above, seven experimentally investigated tests are numerically analysed. The first group of tests includes specimens by Zhao and Yuan [11] of the flexural behaviour of steel-concrete composite beams. The beams consisted of the welded steel I section and concrete slab. The section sizes of steel beams satisfied the Eurocode 4 requirements for compact sections. The cross-sectional data and used material properties are given in Tables 1 and 2, respectively. Variable meanings are given in Figure 1(a) with $b_{ft} = b_{fb} = b_f$ and $t_{ft} = t_{fb} = t_f$.

Figure 7 contains comparison between experimentally and numerically obtained results for the moment-curvature relations. In addition, for tests SCB2, SCB3, and SCB6, the results of the analytical section analysis method by Ban and Bradford [5] are depicted. The results show very good correlation between the experimentally obtained results and results obtained by the presented numerical method. It is expected that even better correlation could be achieved with steel material models that have gradual transition between elastic and plastic regions (e.g., generalized plasticity models [23]).

The second group of tests refers to the experimental research programme performed by Stark [16] at the TNO-IBBC Institute. The tests on small-scale beams and non-ductile block-type connectors are numerically performed. In all tests, beams are constructed as propped. Table 1 contains data about cross-sectional dimensions, and Table 2 contains data about material properties. The results of the experimentally and numerically obtained bending moment resistance for the corresponding degree of shear connection are shown in Figure 8. Again, there is a good agreement between the experimental and numerical results. The numerical results are on the safe side since it completely neglects the slip at the steel section (concrete slab interface).

Table 1: Cross-sectional data for experimental studies [11, 16].

Test name	b_c (mm)	h_c (mm)	d (mm)	b_f (mm)	t_f (mm)	t_w (mm)
SCB1, 2, 3	600	100	150	130	10	10
SCB6	600	100	200	130	10	10
D1, D2, D3	500	40	80	46	5.2	3.8

Table 2: Material properties for experimental studies [11, 16].

Test name	f_c (MPa)	f_{yr} (MPa)	f_y (MPa)	f_u (MPa)	$\mu_1\varepsilon_y$	$\mu_2\varepsilon_y$
SCB1	34.4	338.0	340.7	390.0	0.02	0.14
SCB2	35.2	338.0	450.0	481.0	0.02	0.14
SCB3	74.9	338.0	450.0	481.0	0.02	0.14
SCB6	76.8	338.0	450.0	481.0	0.02	0.14
D1, D2, D3	32.0	—	292.0	292.0	0.02	0.20

5. Parameter Study

As the main goal of the study presented in the paper is to investigate the difference between the nonlinear bending resistance- degree of shear connection relation and a simplified bilinear approximation of this relation, the parameter analysis is performed. The numerical model from the previous section is adjusted to the Eurocode 4 guidelines. However, the conclusions of the study are general and not limited only to the Eurocode 4 design code.

According to Eurocode 4, in the nonlinear section analysis, the parabola-rectangle stress-strain relation for concrete should be used (Figure 9(a)). For the reinforcement, the elastic-linear hardening stress-strain relation is adopted (Figure 9(b)), and the bilinear stress-strain relation without hardening is assumed for the constructional steel. In order to investigate the effect of different material properties, creep effect, method of construction, and reinforcement on the cross-sectional sagging bending resistance, nine different cross sections are analysed. Table 3 contains data about cross-sectional dimensions. As can be seen, the sections are chosen to have a large variety of breadth of the concrete slab, from 60 cm to 300 cm. Sections 4–6, 8, and 9 are the same as in the study by Ban and Bradford [5].

For each cross section, the class of concrete varied among the following classes C25/30, C30/37, C35/45, C40/50, C45/55, and C50/60 with properties given in Table 4. Here, f_{ck} is the characteristic compressive cylinder strength of concrete at 28 days, and E_{cm} is the secant modulus of elasticity of concrete.

Similarly, the study considered the following constructional steel classes: S235, S275, S355, and S450 with yield and ultimate strength values reported in Table 5. Young's modulus of steel is taken as $E_a = 210$ GPa.

For the unpropped constructional method, the following values of the bending moment acting on the steel section alone, M_a, are considered 10%, 20%, 30%, 40%, and 50% of the $M_{a,pl,Rd}$ (plastic moment resistance of steel section only).

Therefore, a total of 1296 numerical section analyses are performed in this part of the study. For each section analysis, the differences between the nonlinear solution and the linear approximation are calculated as follows:

$$\text{difference}\,[\%] = \frac{\eta_{\text{nonlinear}} - \eta_{\text{linear}}}{\eta_{\text{nonlinear}}} \cdot 100, \tag{12}$$

and maximal differences are reported. These results are shown in Figure 10, for both propped and unpropped construction methods. As marked in the figure, the maximal difference for the propped constructional method is 26.1% for Section 9 with concrete class C45/55 and steel S235. The nonlinear and linear solutions for this cross section are shown in Figure 11(a). Also, the case with the best agreement (smallest maximal difference of 3.7%) is shown in Figure 11(b), for Section 3 with concrete class C35/45 and steel S450.

For the unpropped construction method, the maximal differences are larger and go up to 51.5% for Section 9 with concrete class C50/60, steel S235, and the biggest-considered bending moment $M = 50\%$ of $M_{a,pl,Rd}$. The nonlinear solution and the linear solution for this cross section are shown

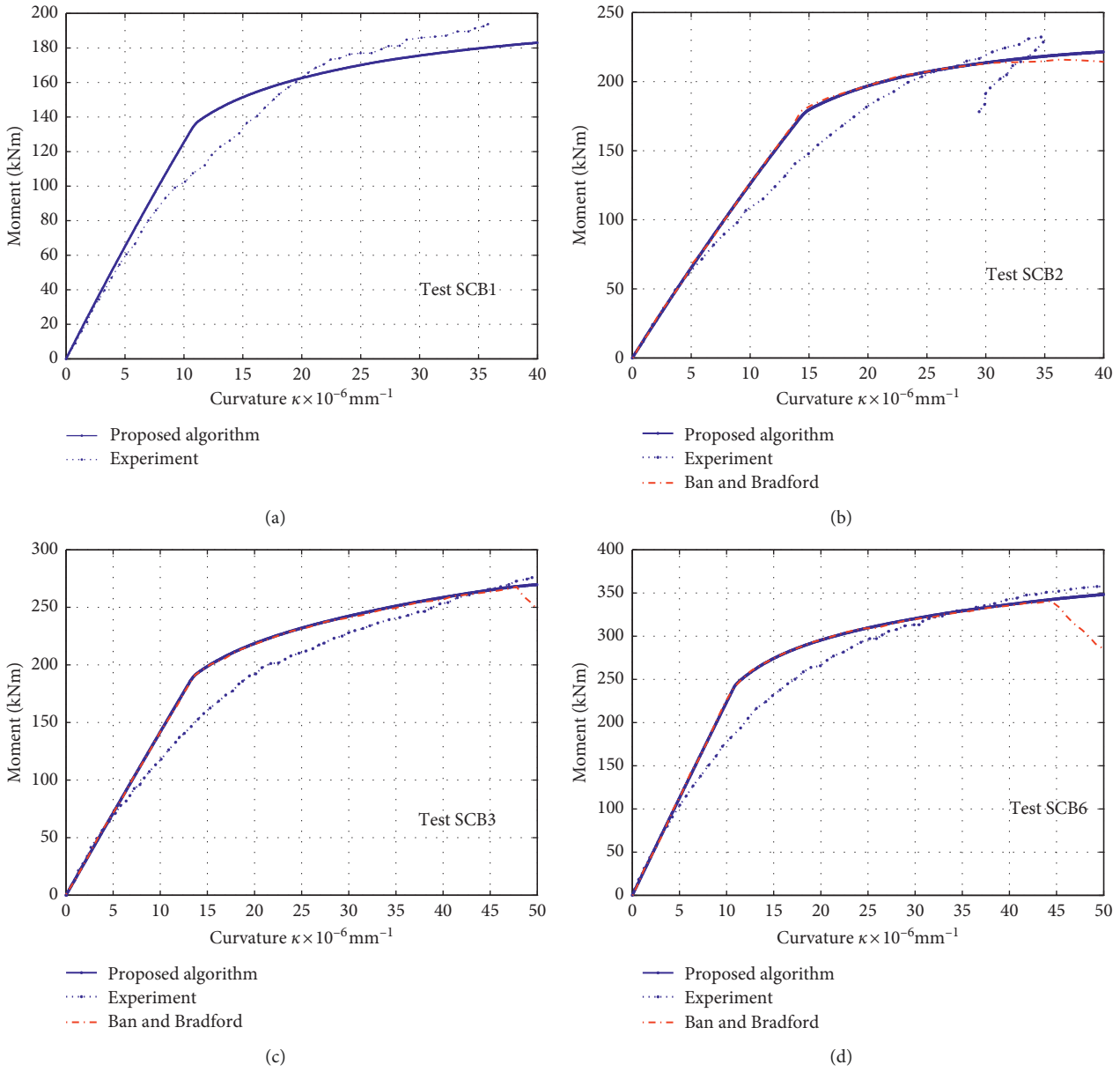

Figure 7: Moment-curvature relations for tests by Zhao and Yuan [11].

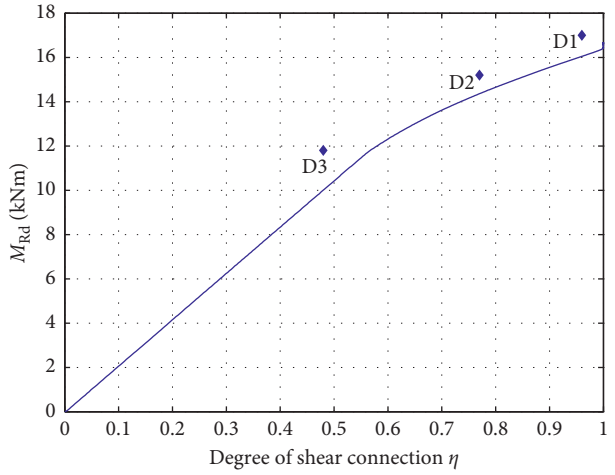

Figure 8: Numerically obtained bending moment-degree of shear connectors relation and experimental results for tests D1, D2, and D3 by Stark [16].

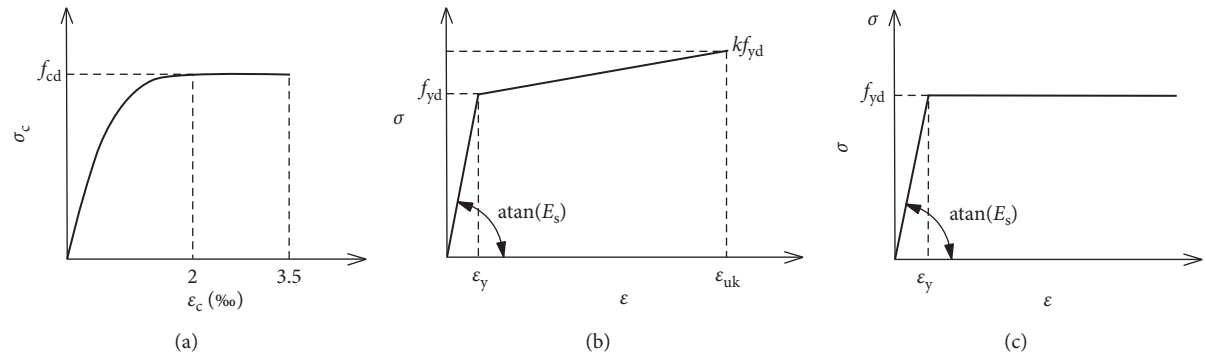

Figure 9: Constitutive relations for (a) concrete, (b) reinforcement, and (c) steel.

Table 3: Parameter study (cross-sectional data).

Section name	b_c (mm)	h_c (mm)	d (mm)	b_f (mm)	t_f (mm)	t_w (mm)
Section 1	600	100	150	130	10	10
Section 2	600	100	200	130	10	10
Section 3	800	100	400	180	13.5	8.6
Section 4	1200	100	300	150	16	12
Section 5	1500	100	450	200	18	14
Section 6	2000	120	600	250	20	16
Section 7	2000	150	384	180	12	8
Section 8	2500	150	750	300	25	20
Section 9	3000	180	900	400	30	25

Table 4: Parameter study (concrete classes).

Concrete class	C25/30	C30/37	C35/45	C40/50	C45/55	C50/60
f_{ck} (MPa)	25	30	35	40	45	50
E_{cm} (GPa)	31	33	34	35	36	37

Table 5: Parameter study (steel classes).

Steel class	S235	S275	S355	S450
f_y (MPa)	235	275	355	440
f_u (MPa)	360	430	510	550

in Figure 12(a), while Figure 12(b) shows the solution for the case with the best agreement (maximal difference of 3.7%) for Section 3, with concrete class C30/37, steel S450, and bending moment $M = 10\%$ of $M_{a,pl,Rd}$.

The results have shown that the maximal difference for unpropped structures is almost double of the value for propped structures, and it increases with increasing bending moment acting on the steel section. Also, in general, the differences are higher for bigger cross sections (larger width of concrete slab and depth of the steel section).

5.1. Variation of Concrete Class. The effect of concrete strength on the bending resistance is investigated next. The typical results for moment resistance curves with the same steel section and variation of concrete class, for the propped constructional method, are shown in Figure 13(a) and for the unpropped constructional method, are shown in Figure 14(a). These figures show results for Section 6 and steel S235.

For unpropped construction, bending moment acting on the steel beam is $M = 50\%$ of $M_{a,pl,Rd}$. Results for Section 7 (shown in Figure 13(b) for propped and in Figure 14(b) for unpropped construction) are different in a way that increment in strength with higher concrete classes is minor. This is because the depth of the steel section is small in comparison with size of the concrete slab. Therefore, the arm of force is small, so stress increment in concrete slab does not produce significant bending moment increment.

5.2. Variation of Steel Class. The effect of the variation of steel class on the resisting bending moment-degree of shear connection relation is shown in Figure 15 for propped and in Figure 16 for unpropped structures. Again, results for Section 6 (Figures 15(a) and 16(a)) and Section 7 (Figures 15(b) and 16(b)) are presented. Evidently, the bending resistance significantly increases with the use of higher steel classes. This increment in strength is more pronounced than when concrete class is varied.

In the case of unpropped structures, the plastic moment resistance of steel section $M_{a,pl,Rd}$ also changes with the steel class, as well as the moment acting on the steel section ($M = 50\%$ of $M_{a,pl,Rd}$ in Figure 16) and curves do not pass through the same point for $\eta = 0$.

5.3. Creep of Concrete Effect. In the described nonlinear section analysis, creep of concrete is taken into account in the first, linear part of the curve, up to $M_{el,Rd}$. This is done, as suggested by Eurocode 4, using the modular ratio η_L for the concrete

$$n_L = n_0 \left(1 + \psi_L \varphi_t\right), \tag{13}$$

where n_0 is the modular ratio E_a/E_{cm} for short-term loading; φ_t is the creep coefficient; ψ_L is the creep multiplied depending on the type of loading. Eurocode 4, in some cases, allows further simplification for building structures and the use of constant value $n_L = 2n_0$. In general, the differences in $M_{el,Rd}$ calculated with n_L from Equation

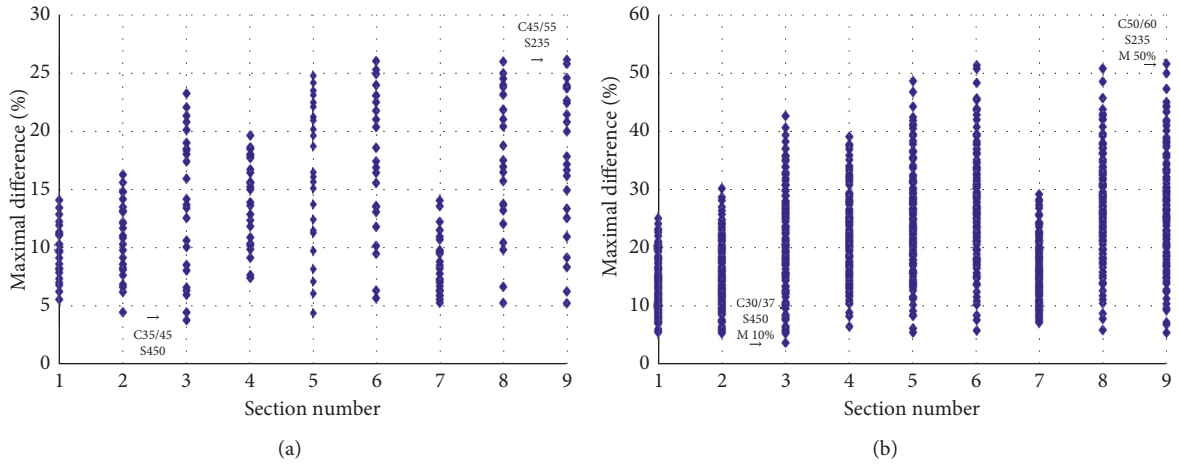

Figure 10: Maximal differences between nonlinear and linear solutions. (a) Propped constructional method and (b) unpropped constructional method.

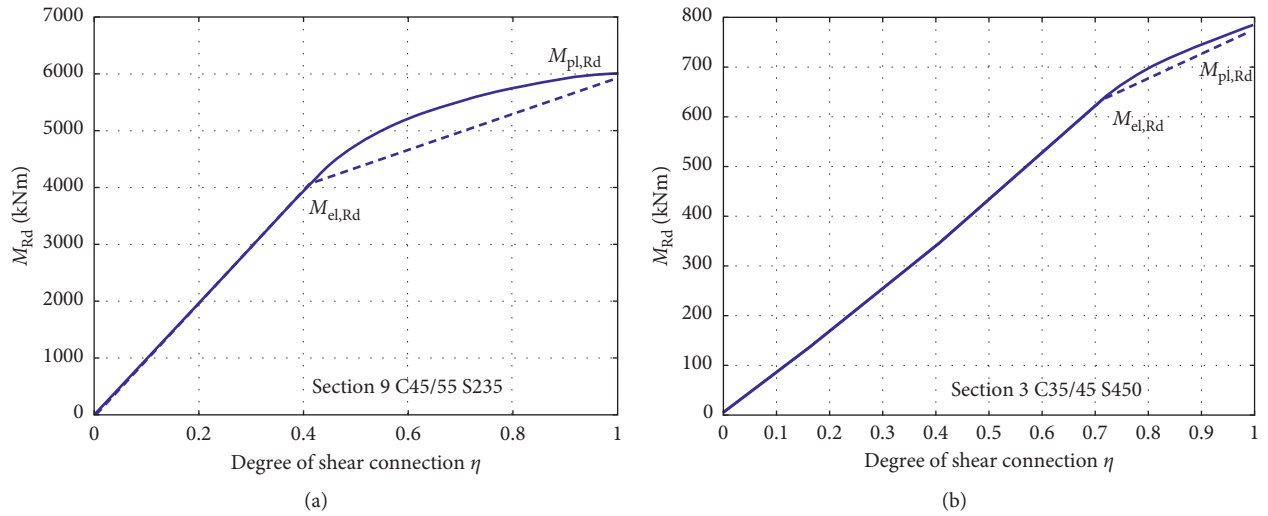

Figure 11: Nonlinear and linear bending moment curve (propped constructional method). (a) Maximal difference (Section 9 C45/55 S235) and (b) minimal difference (Section 3 C35/45 S450).

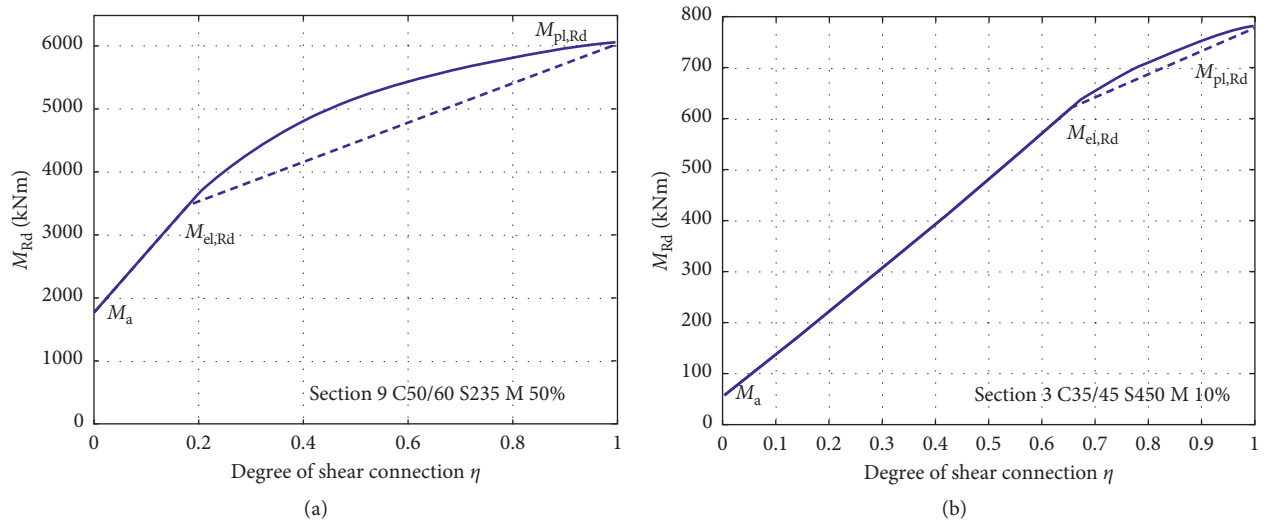

Figure 12: Nonlinear and linear bending moment curve (unpropped constructional method). (a) Maximal difference (Section 9 C50/60 S235 $M = 50\%$) and (b) minimal difference (Section 3 C35/45 S450 $M = 10\%$).

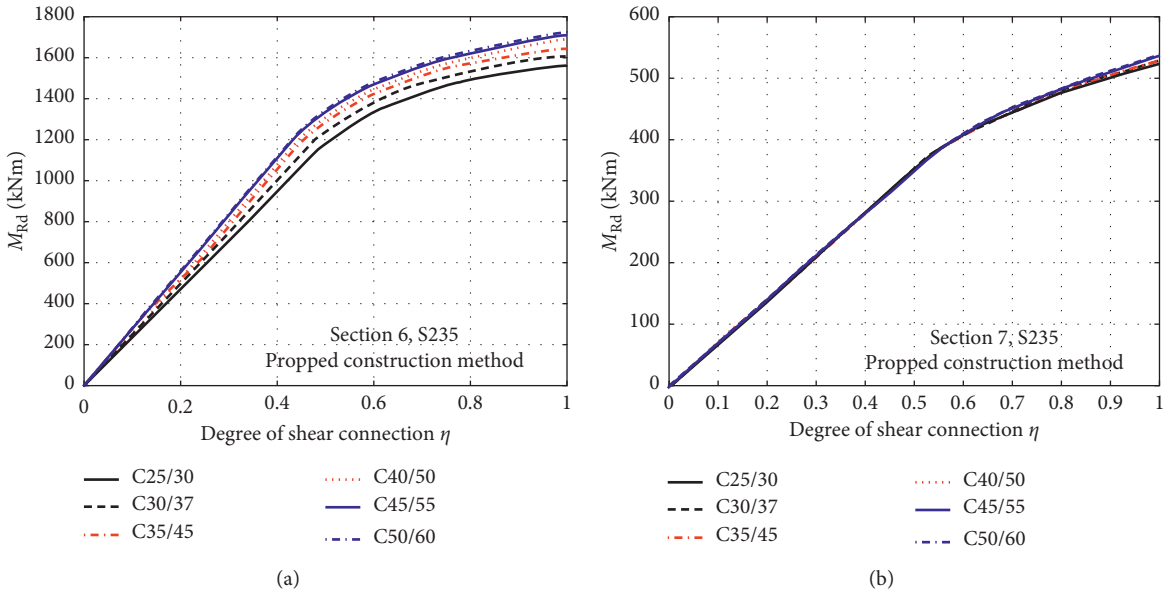

FIGURE 13: Effect of variation of class of concrete on resisting bending moment (degree of shear connection relation). Propped construction method. (a) Section 6 S235 and (b) Section 7 S450.

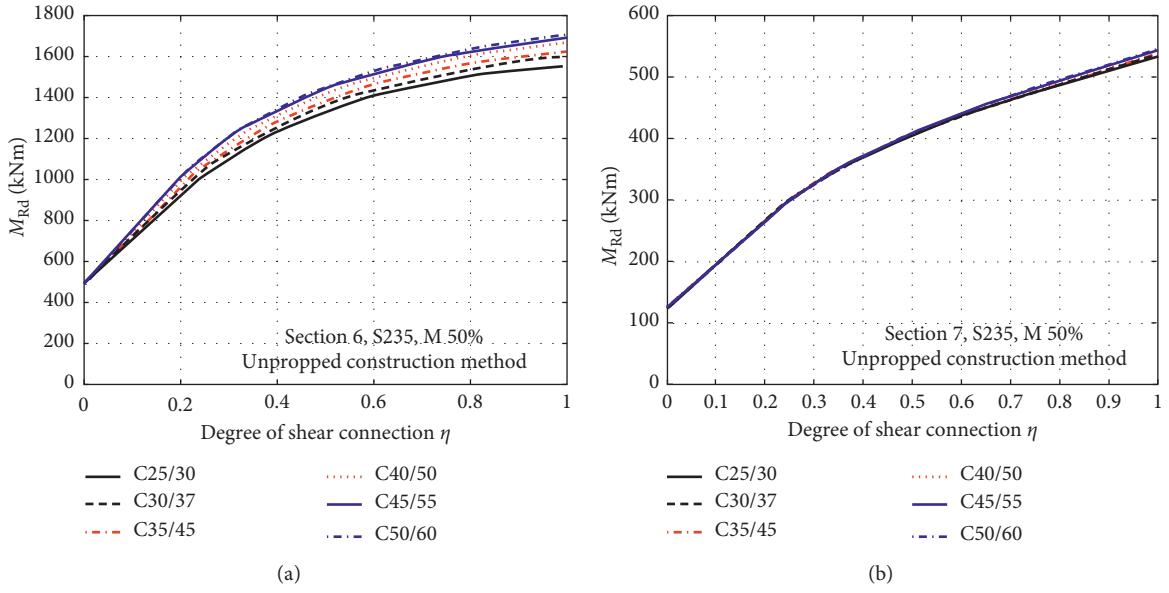

FIGURE 14: Effect of variation of class of concrete on resisting bending moment (degree of shear connection relation). Unpropped construction method. (a) Section 6 S235 M50% and (b) Section 7 S235 M50%.

(13) or with $n_L = 2n_0$ are not significant. Also, this part of the resisting bending moment-degree of shear connection curve corresponds to low degrees of the shear connection which is not of interest. Therefore, the value $n_L = 2n_0$ can be used in the analysis whenever design code (Eurocode 4) rules allow it.

5.4. Concrete Slab Reinforcement. Finally, the study analysed influence of the concrete slab reinforcement on the bending resistance-degree of shear connection relation. The results confirmed the statement that, for sagging bending moment, changes in the bending resistance are insignificant. Just to illustrate this, results for Section 3 C35/45 S275 with and without two reinforcement layers of area 3.925 cm^2, positioned 2 cm and 8 cm from the top of the concrete slab, are shown in Figure 17.

6. Conclusions

The paper presents the nonlinear fiber section analysis for composite steel-concrete cross sections with nonductile

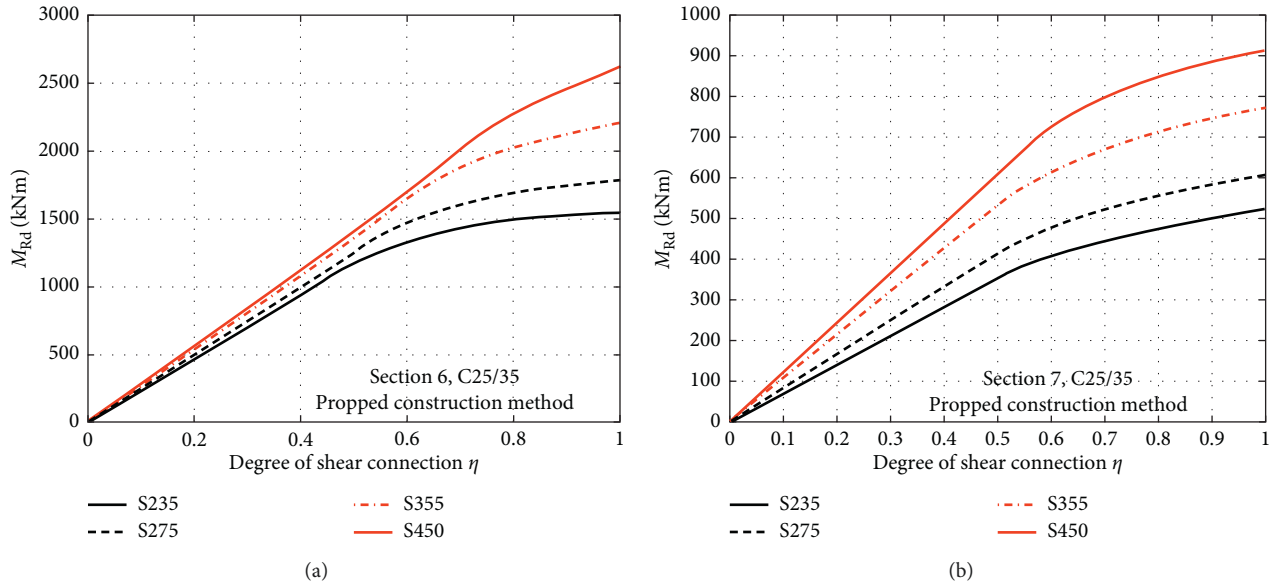

Figure 15: Effect of variation of class of steel on resisting bending moment-degree of shear connection relation (propped construction method). (a) Section 6 C25/35 and (b) Section 7 C25/35.

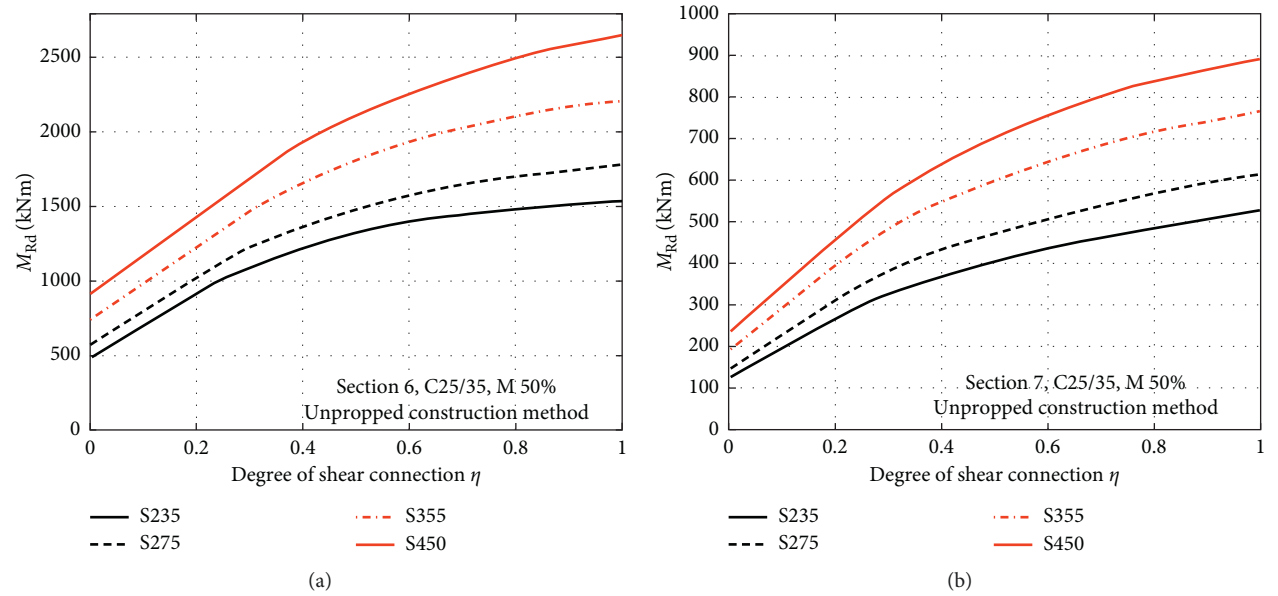

Figure 16: Effect of variation of class of steel on resisting bending moment-degree of shear connection relation. Unpropped construction method. (a) Section 6 C25/35 M50% and (b) Section 7 C25/35 M50%.

shear connectors and partial shear connection. In the analysis, any uniaxial nonlinear material model can be used for constructional steel section, concrete slab, and reinforcement bars. The accuracy of the analysis is verified on few experimental results.

The presented section analysis is used in the parameter study in order to evaluate different methods proposed by design codes for calculation of the bending moment resistance of composite cross sections with nonductile shear connectors and different degrees of shear connection. The following effects are studied: method of construction, variation of concrete class, variation of steel class, presence of slab reinforcement, and creep in the concrete slab. Nine different cross section geometries are included into the analysis.

For the propped construction method, the results showed that the biggest difference between the nonlinear and the bilinear approximation of the relation between the bending moment resistance and degree of shear connection goes up to 26%. Therefore, keeping in mind the simplicity of the bilinear relation, this method is of acceptable accuracy for practical application. However, for unpropped

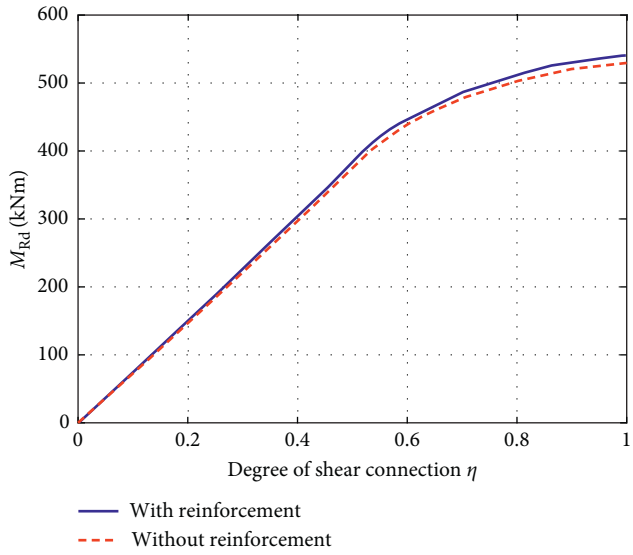

Figure 17: Resisting bending moment-degree of shear connection relation with and without taking into account reinforcement in the concrete slab, Section 3 C35/45 S275.

constructions, this error increases up to around 51%, depending on the value of the bending moment applied on the steel section alone. The bigger the bending moment applied on steel section, the bigger the error. Therefore, results of the approximate method may be over conservative for unpropped structures.

Referring to the variation of the material properties, the study has shown that properties of the constructional steel (yield strength) have more significant influence on the bending resistance moment than strength of the concrete slab. Also, the study has shown that slab reinforcement can be ignored when determining the sagging bending moment resistance.

In the analyses proposed by the codes, creep, taken into account through the modular ratio n_L, effects only the elastic moment resistance $M_{\text{el,Rd}}$ and not the nonlinear part of the M_{Rd}-η curve. It is concluded that the satisfactory results can be obtained using the value $n_L = 2n_0$ when calculating the bending moment resistance.

Data Availability

The data used to support the findings of this study are available from the corresponding author upon request.

Conflicts of Interest

The authors declare that there are no conflicts of interest regarding the publication of this paper.

Acknowledgments

Svetlana M. Kostic thanks the Ministry of Science of Republic of Serbia for financial support under the project number TR36046.

References

[1] D. J. Oehlers and M. A. Bradford, *Elementary Behaviour of Composite Steel and Concrete Structural Members*, Butterworth-Heinemann, London, UK, 2000.

[2] R. P. Johnson, *Composite Structures of Steel and Concrete: Beams, Slabs, Columns and Frames for Buildings*, Blackwell publishing, Hoboken, NJ, USA, 3rd edition, 2004.

[3] X. Xu and Y. Liu, "Load capacities of steel and concrete composite bridge deck slab with haunch," *Advances in Civil Engineering*, vol. 2017, Article ID 3295303, 15 pages, 2017.

[4] C. G. Chiorean and S. M. Buru, "Practical nonlinear inelastic analysis method of composite steel-concrete beams with partial composite action," *Engineering Structures*, vol. 134, pp. 74–106, 2017.

[5] H. Ban and M. A. Bradford, "Elastoplastic cross-sectional behavior of composite beams with high-strength steel: analytical modeling," *Journal of Structural Engineering*, vol. 141, no. 10, pp. 1–12, 2015.

[6] S. J. Hicks and A. Pennington, "Partial factors for the design resistance of composite beams in bending," *Journal of Constructional Steel Research*, vol. 105, pp. 74–85, 2015.

[7] A. Ayoub and F. C. Filippou, "Mixed formulation of nonlinear steel-concrete composite beam element," *Journal of Structural Engineering*, vol. 126, no. 3, pp. 371–381, 2000.

[8] N. Molenstra and R. P. Johnson, "Partial shear connection in composite beams for buildings," *Proceedings of the Institution of Civil Engineers*, vol. 91, no. 4, pp. 679–704, 1991.

[9] J. Turmo, J. A. Lozano-Galant, E. Mirambell, and D. Xu, "Modeling composite beams with partial interaction," *Journal of Constructional Steel Research*, vol. 114, pp. 380–393, 2015.

[10] W. H. Siu and R. K. L. Su, "Analysis of side-plated reinforced concrete beams with partial interaction," *Computers and Concrete*, vol. 8, no. 1, pp. 71–96, 2011.

[11] H. Zhao and Y. Yuan, "Experimental studies on composite beams with high-strength steel and concrete," *Steel and Composite Structures*, vol. 10, no. 5, pp. 373–383, 2010.

[12] L. Zhu and R. K. L. Su, "Analytical solutions for composite beams with slip, shear-lag and time-dependent effects," *Engineering Structures*, vol. 152, pp. 559–578, 2017.

[13] A. Dall'Asta and A. Zona, "Non-linear analysis of composite beams by a displacement approach," *Computers & Structures*, vol. 80, no. 27–30, pp. 2217–2228, 2002.

[14] F. D. Queiroz, P. C. G. S. Vellasco, and D. A. Nethercot, "Finite element modelling of composite beams with full and partial shear connection," *Journal of Constructional Steel Research*, vol. 63, no. 4, pp. 505–521, 2007.

[15] M. Classen, A. Stark, and J. Hegger, "Steel-HSC composite beams with partial shear connection and miniaturized limited-slip-capacity connectors," *Steel Construction*, vol. 11, no. 1, pp. 94–103, 2018.

[16] J. W. B. Stark, "Composite steel and concrete beams with partial shear connection," *Heron*, vol. 34, no. 4, pp. 1–63, 1989.

[17] S. M. Kostic and F. C. Filippou, "Section discretization of fiber beam-column elements for cyclic inelastic response," *Journal of Structural Engineering*, vol. 138, no. 5, pp. 592–601, 2012.

[18] M. Classen, "Limitations on the use of partial shear connection in composite beams with steel T-sections and uniformly spaced rib shear connectors," *Journal of Constructional Steel Research*, vol. 142, pp. 99–112, 2018.

[19] M. Crisinel, "Partial-interaction analysis of composite beams with profiled sheeting and non-welded shear connectors,"

Journal of Constructional Steel Research, vol. 15, no. 1-2, pp. 65–98, 1990.

[20] D. J. Oehlers, N. T. Nguyen, M. Ahmed, and M. A. Bradford, "Partial interaction in composite steel and concrete beams with full shear connection," *Journal of Constructional Steel Research*, vol. 41, no. 2, pp. 235–248, 1997.

[21] R. P. Johnson, *Designers' Guide to EN 1994-1-1 EUROCODE 4: Design of Composite Steel and Concrete Structures Part 1.1: General Rules and Rules for Buildings, Designers' Guide to the Eurocodes*, Thomas Telford Publishing, London, UK, 2012.

[22] E. C. f. Standardization, "Part 1-1: general rules and rules for buildings," in *Eurocode 4, Design of Composite Steel and Concrete Structures: EN 199(4)-1-1*, Thomas Telford Publishing, London, UK, 1992.

[23] F. Auricchio and R. L. Taylor, "Two material models for cyclic plasticity: nonlinear kinematic hardening and generalized plasticity," *International Journal of Plasticity*, vol. 11, no. 1, pp. 65–98, 1995.